Intensification of Pacific storm track linked to Asian pollution

Renyi Zhang, Guohui Li, Jiwen Fan, Dong L. Wu, and Mario J. Molina

PNAS published online Mar 20, 2007;
doi:10.1073/pnas.0700618104

Intensification of Pacific storm track linked to Asian pollution

Renyi Zhang*†, Guohui Li*, Jiwen Fan*, Dong L. Wu‡, and Mario J. Molina†§

*Department of Atmospheric Sciences, Texas A&M University, College Station, TX 77843; ‡ Microwave Atmospheric Sciences, Jet Propulsion Laboratory, California Institute of Technology, Pasadena, CA 91109; and §Department of Chemistry and Biochemistry, University of California at San Diego, La Jolla, CA 92093

Contributed by Mario J. Molina, January 23, 2007 (sent for review January 7, 2007)

Indirect radiative forcing of atmospheric aerosols by modification of cloud processes poses the largest uncertainty in climate prediction. We show here a trend of increasing deep convective clouds over the Pacific Ocean in winter from long-term satellite cloud measurements (1984–2005). Simulations with a cloud-resolving weather research and forecast model reveal that the increased deep convective clouds are reproduced when accounting for the aerosol effect from the Asian pollution outflow, which leads to large-scale enhanced convection and precipitation and hence an intensifed storm track over the Pacific. We suggest that the wintertime Pacific is highly vulnerable to the aerosol–cloud interaction because of favorable cloud dynamical and microphysical conditions from the coupling between the Pacific storm track and Asian pollution outflow. The intensified Pacific storm track is climatically significant and represents possibly the first detected climate signal of the aerosol–cloud interaction associated with anthropogenic pollution. In addition to radiative forcing on climate, intensification of the Pacific storm track likely impacts the global general circulation due to its fundamental role in meridional heat transport and forcing of stationary waves.

aerosols | climate | clouds

Atmospheric aerosols influence cloud development, duration, or precipitation (1–6). This process, known as the aerosol indirect effect, alters the cloud albedo and exerts an important radiative forcing on climate (2). Current understanding of the aerosol indirect effect remains highly uncertain, constituting the greatest uncertainty in climate prediction (2). Cloud processes are determined by complex thermodynamic, dynamical, and microphysical processes and their interactions (5). Following the pioneer work by Twomey (1), there has been accumulative evidence in support of the qualitative conclusion that high aerosol levels reduce the cloud droplet size for a fixed liquid water content (6, 7). Reduced cloud droplet sizes delay the onset of precipitation, leading to invigoration and restructuring of clouds. Measurements of heavy smoke forest fires in the Amazon found suppression of low-level rainout and aerosol washout, which allows transport of water and smoke to upper levels, causing more intensive thunderstorms and release of more latent heat higher in the atmosphere (7). Recent analyses of satellite measurements of the aerosol optical depth and cloud top pressure also suggested a correlation between the presence of aerosols and the structural properties of clouds, indicating a likely cloud invigoration by pollution (8). In addition, enhanced deep convection and mixed-phase processes associated with urban pollution have been implicated in elevated electrification and lightning activities in thunderstorms (9–11).

Increasing pollution levels in Asia and associated outflows have raised considerable concerns because of their potential impact on regional and global climate (12, 13). Notable decadal changes in regional aerosol optical depths during winter months in Asia have been observed from satellite Total Ozone Mapping Spectrometer (TOMS) measurements (14) and can be attributed to dramatically increased SO_2 and soot emissions from fossil-fuel burning. In this report, we present an analysis of long-term satellite cloud measurements, emphasizing the north Pacific region, where most transPacific pollution transport occurs (15).

Results and Discussion

The data used in this study are monthly mean cloudiness from the International Satellite Cloud Climatology Project (ISCCP), which contains a long-term record with a global coverage. The ISCCP data correspond to cloud statistics from 1984 to 2005 and are derived by using all operational geostationary and polar orbiting weather satellites (16). The data are a merger of advanced very high-resolution radiometer polar orbiter data two to four times per day, with available geosynchronous observations superimposed. The ISCCP uses the channels common to weather satellites, the visible channel at 0.6 μm and the infrared window at 11 μm, to detect clouds and measure their optical depths. We considered deep convective clouds (DCCs) from the ISCCP data, classified by the measured values of the cloud optical thickness (23–379) and cloud top pressure (440–50 mbar). Comparison of the amount of optically thick clouds between ISCCP and high-resolution infrared sounder (HIRS) showed a good agreement (17) [see supporting information (SI) *Text*].

Figure 1 displays January distributions of ISCCP DCC amounts averaged during the periods of 1984–1993 and 1994–2005. A prominent feature over the Pacific Ocean lies in the relatively high DCC amounts (Fig. 1 *a* and *b*), which extend mostly from southwest to northeast. The DCC pattern coincides with the winter Pacific storm track. Over the northwest Pacific, the near-surface meridional temperature gradient is high in midlatitudes, where the cold, dry, monsoonal air encounters the warm air mass to the south. Also, there is an abundant supply of heat and moisture from the warm ocean surface to the monsoonal air. The two effects sustain high lower tropospheric baroclinicity, which facilitates migrating baroclinic eddies to form a storm track downstream (18), characterized by a belt of local maximal precipitation across almost the entire north Pacific (19). The Pacific storm track is fundamental to the global general circulation by relaxing the Earth's temperature gradient through sensible heat transport to higher latitudes and the forcing of stationary waves (18).

Author contributions: R.Z. designed research; R.Z., G.L., and J.F. performed research; R.Z., G.L., D.L.W., and M.J.M. analyzed data; and R.Z. wrote the paper.

The authors declare no conflict of interest.

Freely available online through the PNAS open access option.

Abbreviations: TOMS, Total Ozone Mapping Spectrometer; ISCCP, International Satellite Cloud Climatology Project; DCC, deep convective cloud; HIRS, high-resolution infrared sounder; CR-WRF, cloud-resolving weather research and forecasting.

†To whom correspondence may be addressed. Email: zhang@ariel.met.tamu.edu or mjmolina@ucsd.edu.

This article contains supporting information online at www.pnas.org/cgi/content/full/0700618104/DC1.

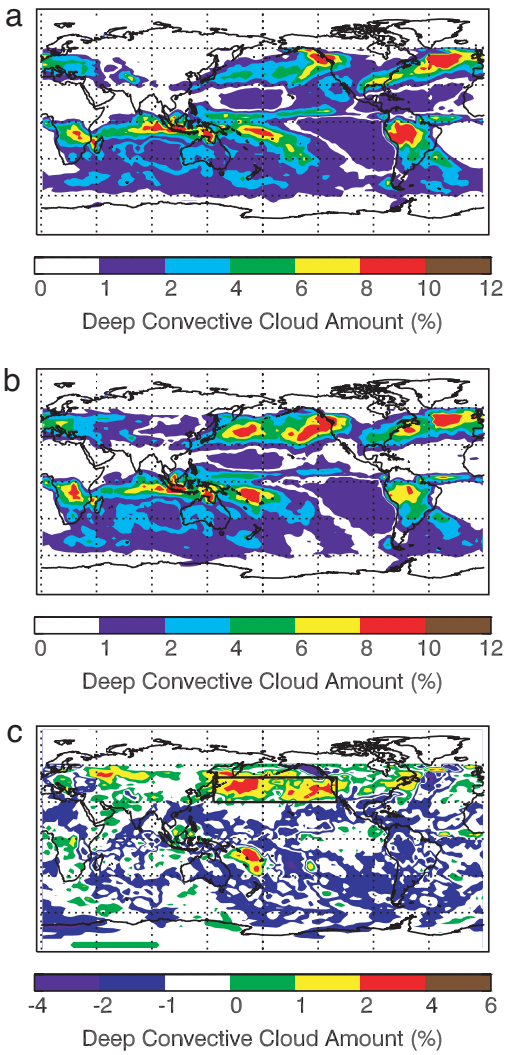

Fig. 1. Global cloud measurements from ISCCP. The January distribution of deep convective cloud amounts from ISCCP averaged over the periods of 1984–1994 (*a*) and 1994–2005 (*b*). (*c*) Difference between *b* and *a*, i.e., *b* − *a*. The cloud amount is defined as the ratio of the number of cloudy pixels to the total number of image pixels within the map grid cell (16). The black box in *c* marks the north Pacific region with latitudes from 30N to 50N and longitudes from 140E to 230W.

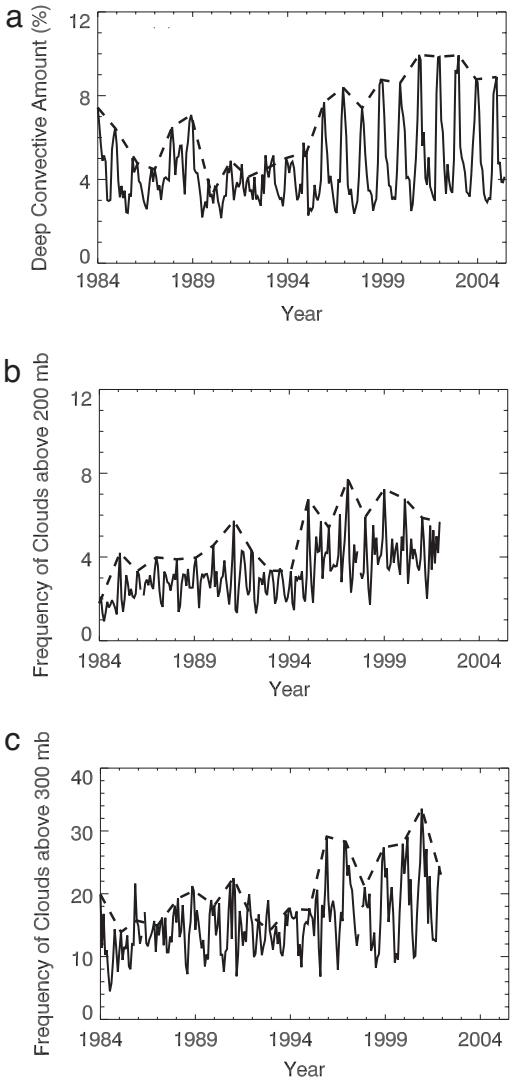

Fig. 2. Time series of cloud measurements from 1984–2005. The time series of deep convective cloud amounts from ISCCP (*a*) and frequencies of high clouds above 200 mbar (*b*) and 300 mbar (*c*) from HIRS averaged over the entire north Pacific, i.e., latitudes from 30N to 50N and longitudes from 140E to 230W (as labeled in the black box in Fig. 1*c*). The dotted line corresponds to the maximum wintertime (December–February) values.

A comparison between the periods of 1984–1994 and 1994–2005 shows a considerable increase in the DCC amount (by ≈20–50%) over much of the north Pacific (Fig. 1 *b* and *c*). The DCC enhancement also exhibits a similar pattern to the storm track and is mostly evident over the northwest Pacific (Fig. 1 *b* and *c*), where a local maximum in the climatological-mean precipitation exists (19). The time series of the DCC amount averaged over the north Pacific reveals seasonal and interannual variability (Fig. 2*a*). The DCC amount typically reaches a maximum in December/January associated with an active storm track and attains a minimum in July/August because of suppressed deep convection by the summer Pacific high. A marked trend of increasing wintertime DCCs occurred after the mid-1990s and reached a peak between 2001 and 2003. We also analyzed cloud measurements from HIRS and found a similar trend of increased wintertime high clouds over the north Pacific (Fig. 2 *b* and *c*). Notice that there is little variation in the DCC amount over the north Atlantic, where a storm track also exists during the winter period.

An examination of the sea surface temperature over the north Pacific reveals little correlation between the sea surface temperature and DCC trends in winter (SI Fig. 5), excluding a plausible thermodynamic cause for the enhanced DCC trend. Although there is evidence of the storm track response to the El Niño southern oscillation (20, 21), the cloud data with a 10-year average (Fig. 1*c*) are insensitive to this effect (with a typical frequency of ≈2–4 years). The Pacific storm track activity has also been shown to exhibit interannual and decadal variabilities, which may correlate with modulations of the east Asian winter monsoon and associated meridional heat transport (21). A decadal tendency of an enhanced storm track activity in mid-winter over the northwest Pacific has been attributed to the decadal weakening of the east Asian winter monsoon (Siberian high) and the Aleutian low that occurred in the late 1980s (21). These observed modulations, however, appear to be incompatible to the trend of increasing DCC amounts since mid-1990s. Furthermore, the DCC trend does not show a correlation with other low-level cloud types or the total cloud coverage from the

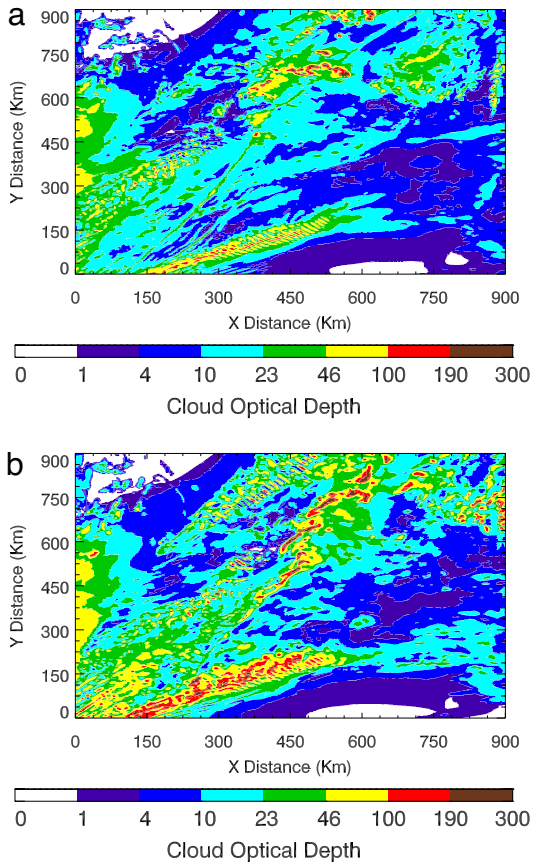

Fig. 3. Model simulations of storms in the Pacific. The CR-WRF simulations of the cloud optical depth for a storm event occurring over the north Pacific on November 30, 2003, from 00 UTC to 12 UTC. The results shown are 10 h after the model initiation. The model domain centers at 38N and 145E. Simulations for marine (*a*) and polluted (*b*) continental aerosol types.

ISCCP data over this region (SI Fig. 6). Hence, the observed trend of increasing DCCs over the Pacific Ocean in winter is unlikely to be due to natural variability.

Rapid industrialization and urbanization in Asia have caused severe air pollution over many countries, including China and India (13). Long-term satellite measurements have revealed a dramatic increase in aerosol concentrations over Asia (14). The analysis of the TOMS aerosol data showed a large increasing trend in the aerosol optical depth over the China coastal plain during the winter months (14), especially over the past decade (SI Fig. 7). The increasing aerosol trend has been explained by SO_2 and soot emissions, with an increase in SO_2 emissions of 35% per decade over the same region (22). Anthropogenic SO_2 and soot emissions in Asia are most important for the regional aerosol budget in the winter months because coal is burned as a main source of heat and energy, whereas dust and boreal fire smoke contributions are minimal during the year (14, 22). The regions in the remote marine troposphere typically contain lower levels of sea-salt and sulfate aerosols (5), as also depicted in the TOMS aerosol measurements during the period of 1984–1994 over the Pacific (SI Fig. 7*a*). Recently elevated long-range transport of anthropogenic aerosols from Asia to the north Pacific by the prevailing westerly wind is clearly evident from satellite measurements by the Multiangle Imaging Spectro Radiometer (23), TOMS, and the Moderate Resolution Imaging Spectroradiometer (SI Figs. 7–9). In particular, transported Asian pollution, including anthropogenic aerosols, has been measured, showing that surface emissions were lifted into the

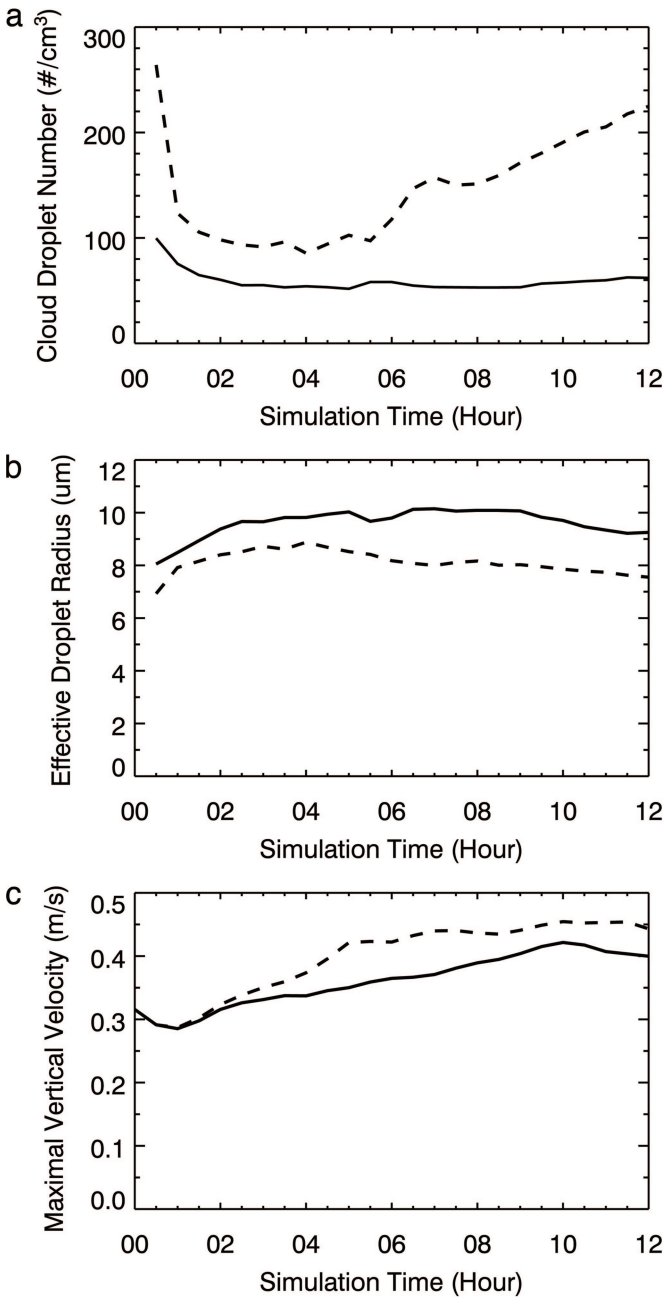

Fig. 4. CR-WRF simulations of cloud properties. The simulated area-mean (over the entire model domain) cloud droplet number concentration (*a*), effective droplet radius (*b*), and maximum vertical velocity (*c*). The solid and dashed curves correspond to the simulations of marine and polluted continental aerosol types, respectively.

free troposphere over Asia and transported to North America in ≈6 days (24).

To evaluate the aerosol–cloud interaction due to the Asian pollution outflow, we performed simulations of wintertime deep convective storms over the northwest Pacific by using a cloud-resolving weather research and forecasting (CR-WRF) model. Two aerosol scenarios were considered on the basis of atmospheric measurements over this region (25): The marine aerosols were assumed to contain mainly NaCl with a number concentration of 400 cm^{-3}, and polluted continental aerosols were assumed to mainly consist of $(NH_4)_2SO_4$ with a concentration of 2,000 cm^{-3}. The CR-WRF experiments with elevated polluted continental

aerosols yielded considerably more DCC development than that predicted with marine aerosols: The DCC amount increased by >40% for the cloud optical depth of >23 over the entire model domain (Fig. 3) because of the increased liquid and ice water path. Thus, the observed DCC enhancement over the north Pacific in winter is reproduced in model simulations that account for the aerosol effect from the Asian pollution outflow.

The north Pacific in winter is highly susceptible to the aerosol effect. The frequent wintertime transient eddies and large lower level tropospheric baroclinicity over this region provide instability for air-parcel lifting and convective development (18). Also, there is an abundant water vapor supply due to evaporation from the oceanic surface that facilitates condensational droplet growth of maritime clouds. Maritime clouds are generally distinct from continental clouds in both dynamical and microphysical characteristics. There is less surface heating for the ocean than for land. Also, maritime clouds typically contain lower droplet concentrations but larger sizes, whereas continental clouds typically contain higher droplet concentrations but smaller sizes (5). The difference in the cloud droplet sizes is explained by the difference in the cloud condensation nuclei (CCN) concentrations between land and ocean. As a result, there exists a major difference in the "colloidal stability" between the two cloud types (26). Maritime clouds precipitate readily by coalescence growth, whereas the warm process is often suppressed in continental clouds, and precipitation often involves mixed-phase processes (i.e., ice particles and supercooled droplets) because of persistent updrafts from released latent heat during droplet condensation and the absence of precipitation-induced downdrafts. Those dynamical and microphysical distinctions are clearly exemplified from observations of a dramatic land–ocean lightning contrast, lesser availability of supercooled water at higher altitudes, weaker updraft velocities, and weaker vertical profiles of radar reflectivity in the mixed-phase region for maritime clouds than for continental clouds (27, 28). Conversely, polluted Asian outflows transport high levels of aerosols throughout the north Pacific (15, 25), a large fraction of which are capable of activating cloud droplets by serving as CCN. Elevated CCN levels increase the cloud droplet concentration and updraft velocity, but reduce the mean droplet size (Fig. 4), leading to suppressed coalescence and warm rain but efficient mixed-phase precipitation (29). In addition, the CR-WRF predicts an increase of about 25% in precipitation over the entire model domain for the polluted Asian aerosol case compared to the marine aerosol case. The changed cloud microphysical processes, along with the favorable baroclinic instability and moisture supply, result in stronger convection and more precipitation on a large scale over the Pacific. Such enhanced convection and precipitation most likely signify an intensified storm track.

Long-term observations and *in situ* measurements of aerosols and cloud microphysical properties over the Pacific are generally very limited. Recent aircraft measurements conducted over the northwest Pacific corroborated the correlation between elevated levels of aerosols and modified cloud microphysical properties (25, 30). The extent of the Asian pollution outflow was discernible from measurements of SO_2 and aerosols outside of a cloud regime. For the case of relatively low background concentrations of SO_2 and aerosols larger droplet sizes but lower concentrations were measured within the cloud, whereas with elevated concentrations of SO_2 and aerosols smaller droplet sizes but higher concentrations were measured (25, 30). Those results indicated that high aerosols and CCN concentrations decreased the effective cloud droplet radius under the Asian pollution outflow. The observational microphysical differences between the clean and polluted cases were consistent with those predicted from the CR-WRF simulations (Fig. 4).

We have identified a trend of increasing DCC over the north Pacific in winter, and we have demonstrated the link between the intensified Pacific storm track and Asian pollution outflow. Our results suggest that the winter Pacific is highly vulnerable to the aerosol effect because of favorable cloud dynamical and microphysical conditions from the interaction between the storm track and Asian pollution outflow. The intensified storms over the Pacific in winter are climatically significant and represent a detected climate signal of the aerosol–cloud interaction associated with anthropogenic pollution. The intensified Pacific storm track likely has profound implications on climate. Intensified storms of the Pacific storm track can significantly alter the cloud albedo and impact the radiative budget over such a large region. An intensified Pacific storm track can also impact the global general circulation because of its fundamental role in meridional and vertical heat transport and forcing of stationary waves (18). In particular, a changed Pacific storm track will inevitably influence the wintertime weather pattern over North America. Furthermore, intensified storms over the Pacific can transfer efficiently anthropogenic aerosols vertically and northward. In particular, efficient polar transport of sensible heat and anthropogenic aerosols can exacerbate warming at higher latitudes. Recent assessments of climate change by the Intergovernmental Panel on Climate Change reveal that the largest warming occurs over the polar regions (2), plausibly linked to changes in snow/ice albedo due to reductions in ice cover and deposition of soot aerosols (31) or feedback of clouds and the hydrological cycle involving aerosols (32). Warming in the polar regions has catastrophic climate consequences, such as polar ice caps shrinking and sea level rising (2, 33). The change in the Pacific storm track and its associated climate impacts require further studies from the scientific community, including investigation with global climate models.

Methods

A two-moment microphysical scheme was incorporated into the WRF model to consider the effects of aerosols on clouds (see also *SI Text*). The microphysical scheme in CR-WRF calculated the mass-mixing ratios and the number concentrations of aerosols and five types of hydrometeors. Various cloud processes were included in the CR-WRF, including both warm and mixed-phase microphysics. We present here simulations of a storm event occurring over the north Pacific on November 30, 2003, from 00 UTC to 12 UT. The storm was identified on the basis of the temperature and wind fields from the National Center for Environmental Predictions/National Center for Atmospheric Research reanalysis. The simulations were performed by using a 3-km horizontal resolution, with a 1,050 × 1,050-km domain centered at 38N and 145E. Initial and boundary conditions in the simulations were taken from WRF standard initialization output by using the National Center for Environmental Predictions/National Center for Atmospheric Research reanalysis 1° × 1° data.

The authors thank Earle Williams, Chunsheng Zhao, and J. Nielsen-Gammon for helpful discussions, and gratefully acknowledge the use of ISCCP, HIRS, Multiangle Imaging Spectro Radiometer, and TOMS database. This work was supported by National Science Foundation Grant ATM-0424885 (to R.Z.). The Jet Propulsion Laboratory is supported by the National Aeronautics and Space Administration, and J.F. was supported by a National Aeronautics and Space Administration fellowship.

1. Twomey SA (1974) *Atmos Environ* 8:1251–1256.
2. Houghton JT (2001) *Intergovernmental Panel on Climate Change Report* (Cambridge Univ Press, New York).
3. Charlson RJ, Lovelock JE, Andreae MO, Warren SG (1987) *Nature* 326:655–661.
4. Zhang R, Suh I, Zhao J, Zhang D, Fortner EC, Tie X, Molina LT, Molina MJ (2004) *Science* 304:1487–1490.
5. Roger RR, Yau MK (1989) *A Short Course in Cloud Physics* (Butterworth–Heinemann, Woburn, MA).
6. Rosenfeld D (2000) *Science* 287:1793–1796.

7. Andrea MO, Rosenfeld D, Artaxo P, Costa AA, Frank GP, Longo KM, Silva-Dias MAF (2004) *Science* 303:1337–1342.
8. Koren I, Kaufman Y, Rosenfeld D, Rimer LA, Rudich Y (2005) *Geophys Res Lett* 32, 10.1029/2005GL023187.
9. Orville RE, Huffines G, Nielsen-Gammon J, Zhang R, Ely B, Steiger S, Philips S, Allen S, Read W (2001) *Geophys Res Lett* 28:2597–2600.
10. Zhang R, Tie X, Bond DW (2003) *Proc Natl Acad Sci USA* 100:1505–1509.
11. Zhang R, Lei W, Tie X, Hess P (2004) *Proc Natl Acad Sci USA* 101:6346–6350.
12. Ramanathan V, Crutzen PJ, Kiehl JT, Rosenfeld D (2001) *Science* 294:2119–2124.
13. Lelieveld J, Crutzen PJ, Ramanathan V, Andreae MO, Brenninkmeijer CAM, Campos T, Cass GR, Dickerson RR, Fischer H, de Gouw JA, *et al*. (2001) *Science* 291:1031–1036.
14. Massie ST, Torres O, Smith SJ (2004) *J Geophys Res* 109, 10.1029/2004JD004620.
15. Liu H, Jacob DJ, Bey I, Yantosca RM, Duncan BN, Sachse GW (2003) *J Geophys Res* 108, 10.1029/2002JD003102.
16. Rossow WB, Schiffer RA (1991) *Bull Amer Meteor Soc* 72:2–20.
17. Jin Y, Rossow WB, Wylie DP (1996) *J Climate* 9:2850–2879.
18. Hoskins BJ, Valdes PJ (1990) *J Atmos Sci* 47:1854–1864.
19. Xie P, Arkin PA (1997) *Bull Amer Meteor Soc* 78:2539–2558.
20. Orlanski I (2005) *J Atmos Sci* 62:1367–1390.
21. Nakamura H, Izumi T, Sampe T (2002) *J Climate* 15:1855–1874.
22. Smith SJ, Pitcher H, Wigley TML (2001) *Global Planet Change* 29: 99–199.
23. Kahn R, Li WH, Martonchik JV, Bruegge CJ, Diner DJ, Gaitley BJ, Abdou W, Dubovik O, Holben B, Smirnov A, *et al*. (2005) *J Atmos Sci* 62:1032–1052.
24. Jaffe D, Anderson T, Covert D, Kotchenruther R, Trost B, Danielson J, Simpson W, Berntsen T, Karlsdottir S, Blake D, *et al*. (1999) *Geophys Res Lett* 26:711–714.
25. Zhao C, Tie X, Brasseur G, Noone KJ, Nakajima T, Zhang Q, Zhang R, Huang M, Duan Y, Li G, Ishizaka Y (2006) *Geophys Res Lett* 33, 10.1029/2006GL026653.
26. Squires P (1958) *Tellus* 10:256–271.
27. Nesbitt SW, Zhang R, Orville RE (2000) *Tellus B* 52:1206–1215.
28. Williams ER, Zhang R, Rydock J (1991) *J Atmos Sci* 48:2195–2203.
29. Fan J, Zhang R, Li G, Tao WK, Li X (2007) *J Geophys Res* 112, 10.1029/2006JO007688.
30. Adhikari M, Ishizaka Y, Minda H, Kazaoka R, Jensen JB, Gras JL (2005) *J Geopshys Res* 110, 10.1029/2004JD004758.
31. Hanson J, Nazarenko L (2004) *Proc Natl Acad Sci USA* 101:423–428.
32. Rinke A, Dethloff K, Fortmann M (2004) *Geophys Res Lett* 31, 10.1029/2004GL020218.
33. Kerr RA (2006) *Science* 311:1698–1701.